10.2514/6.2025-0286

AIAA Science and Technology Forum and Exposition (SciTech 2025), Orlando, FL, January 6-10, 2025

HIGH-FIDELITY DIGITAL TWINS: ZOOMING IN ON WEAKNESSES IN STRUCTURES

Rainald Löhner[1], Facundo Airaudo[1], Harbir Antil[2],
Roland Wüchner[3], Suneth Warnakulasuriya[3], Ihar Antonau[4] and Talhah Ansari[3]

[1] *Center for Computational Fluid Dynamics*
George Mason University, Fairfax, VA 22030-4444, USA
[2] *Center for Mathematics and Artificial Intelligence*
George Mason University, Fairfax, VA 22030-4444, USA
[3] *Chair of Structural Analysis*
TU München, München, Germany
[4] *Institute of Structural Analysis*
TU Braunschweig, Braunschweig, Germany

An adjoint-based procedure to determine weaknesses, or, more generally, the material properties of structures is improved by implementing two techniques to progressively reduce the regions considered as weakened. In this way, the number of degrees of freedom that are being optimized is reduced, leading to faster convergence and a better definition or 'sharpening' of the weakened region.
Several examples show the viability, accuracy and efficiency of the proposed methodology and its potential use for high fidelity digital twins.

I. INTRODUCTION

Given that all materials exposed to the environment and/or undergoing loads eventually age and fail, the task of trying to detect and localize weaknesses in structures is common to many fields. To mention just a few: airplanes, drones, turbines, launch pads and airport and marine infrastructure, bridges, high-rise buildings, wind turbines, and satellites. Traditionally, manual inspection was the only way of carrying out this task, aided by ultrasound, X-ray, or vibration analysis techniques. The advent of accurate, abundant and cheap sensors, together with detailed, high-fidelity computational models in an environment of digital twins has opened the possibility of enhancing and automating the detection and localization of weaknesses in structures.

As the task of damage detection is of such importance, many analytical techniques have been developed over the last decades.[4, 10–12, 18, 20, 25, 26, 28, 29, 32, 33] Some of these were developed to identify weaknesses in structures, others (e.g.[20]) to correct or update finite element models. The damage/weakness detection from measurements falls into the more general class of inverse problems where material properties are sought based on a desired cost functional.[8, 10, 21, 34] It is known that these inverse problems are ill-defined and require regularization techniques.

The analytical methods depend on the measurement device at hand, and one can classify broadly according to them. The first class of analytical methods is based on changes observed in (steady) displacements or strains.[4, 12, 25, 32, 35] The second class considers velocities or accelerations in the time domain.[18, 28, 33] The third class is based on changes observed in the frequency domain.[10, 11, 20, 26, 29]

Some of the methods based on displacements, strains, velocities or accelerations used adjoint formulations[5, 12, 23, 28, 32, 35, 37] in order to obtain the gradient of the cost function with the least amount of effort.

In the present case, the procedures used are also based on measured forces and displacements/strains, use adjoint formulations and smoothing of gradients to quickly localize damaged regions.[2,3,24] Unlike previous efforts, they are intended for weakness/damage detection in the context of digital twins,[1,7,30,38] , i.e. we assume a set of defined loadings and sensors that accompany the structure (object, product, process) throughout its lifetime in order to monitor its state. The digital twins are assumed to contain finite element discretizations/models of high fidelity, something that nowadays is common in the aerospace industry. Therefore, the proposed approach fits well into the overall workflow of high-level CAD environments and high fidelity FEM models seen in the design phase.

II. ASSUMPTIONS

What follows relies on the following set of assumptions:

- Monitoring the weakening of a structure is carried out by applying a set of n different forces $\mathbf{f}_i, i = 1, n$ and measuring the resulting displacements $\mathbf{u}_{ij}^{md}, i = 1, n, j = 1, m$ and/or strains $\mathbf{s}_{ij}^{ms}, i = 1, n, j = 1, m$ at m different locations $\mathbf{x}_j, j = 1, m$ (the intrinsic assumption is that the forces can be standardized and perhaps even maintained throughout the life of the structure);

- The weakening of a structure may occur at any location, i.e. there are no regions that are excluded for weakening; this is the most conservative assumption, and could be relaxed under certain conditions;

- The sensors for displacements and strains are limited in their ability to measure by noise/signal ratios, i.e. actual displacements and strains have to be larger than a certain threshold to be of use:

$$|\mathbf{u}^m| \geq u_0 \quad , \quad |\mathbf{s}^m| \geq s_0 \quad . \tag{2.1}$$

- The type of force used to monitor the weakening of a structure is limited by practical considerations; this implies that the number of different forces is limited, and can not assume arbitrary distributions in space.

- The initial weakening of a structure may be described by a field $\alpha(\mathbf{x})$, where $0 \leq \alpha(\mathbf{x}) \leq 1$ and $\alpha(\mathbf{x}) = 0$ corresponds to total failure (no load bearing capability) while $\alpha(\mathbf{x}) = 1$ is the original state;

- The displacements, strains and stresses of the structure are well described by a sufficiently fine finite element discretization (e.g. trusses, beams, plates, shells, solids),[36,39] which results in a system of equations for each load case:

$$\mathbf{K} \cdot \mathbf{u}_i = \mathbf{f}_i \quad , \quad i = 1, n \tag{2.2}$$

  where $\mathbf{u}_i$ are the displacements and $\mathbf{K}$ the usual stiffness matrix, which is obtained by assembling all the element matrices:

$$\mathbf{K} = \sum_{e=1}^{N_e} \mathbf{K}_e \quad . \tag{2.3}$$

III. DETERMINING MATERIAL PROPERTIES VIA OPTIMIZATION

The determination of material properties (or weaknesses) may be formulated as an optimization problem for the strength factor $\alpha(\mathbf{x})$ as follows: Given n force loadings $\mathbf{f}_i, i = 1, n$ and $n \cdot m$ corresponding measurements at m measuring points/locations $\mathbf{x}_j, j = 1, m$ of their respective displacements $\mathbf{u}_{ij}^{md}, i = 1, n, j = 1, m$ or strains $\mathbf{s}_{ij}^{ms}, i = 1, n, j = 1, m$, obtain the spatial distribution of the strength factor α that minimizes the cost function:

$$I(\mathbf{u}_{1,..,n}, \mathbf{s}_{1,..,n}, \alpha) = \frac{1}{2} \sum_{i=1}^{n} \sum_{j=1}^{m} w_{ij}^{md} (\mathbf{u}_{ij}^{md} - \mathbf{I}_{ij}^{d} \mathbf{u}_i)^2 + \frac{1}{2} \sum_{i=1}^{n} \sum_{j=1}^{m} w_{ij}^{ms} (\mathbf{s}_{ij}^{ms} - \mathbf{I}_{ij}^{s} \mathbf{s}_i)^2 \quad , \tag{3.1}$$

subject to the finite element description (e.g. trusses, beams, plates, shells, solids) of the structure[36,39] under consideration (i.e. the digital twin/system[13,27]):

$$\mathbf{K} \cdot \mathbf{u}_i = \mathbf{f}_i \quad , \quad i = 1, n \tag{3.2}$$

where w_{ij}^{md}, w_{ij}^{ms} are displacement and strain weights, $\mathbf{I}^d, \mathbf{I}^s$ interpolation matrices that are used to obtain the displacements and strains from the finite element mesh at the measurement locations, and $\mathbf{K}$ the usual stiffness matrix, which is obtained by assembling all the element matrices:

$$\mathbf{K} = \sum_{e=1}^{N_e} \alpha_e \mathbf{K}_e \quad , \tag{3.3}$$

where the strength factor α_e of the elements has already been incorporated. We note in passing that in order to ensure that $\mathbf{K}$ is invertible and non-degenerate $\alpha_e > \epsilon > 0$. Note that the optimization problem given by Eqns.(3.1-3.3) does not assume any specific choice of finite element basis functions, i.e. is widely applicable.

3.1 OPTIMIZATION VIA ADJOINTS

The objective function can be extended to the Lagrangian functional

$$L(\mathbf{u}_{1,..,n}, \alpha, \tilde{\mathbf{u}}_{1,..,n}) = I(\mathbf{u}_{1,..,n}, \alpha) + \sum_{i=1}^{n} \tilde{\mathbf{u}}_i^t (\mathbf{K}\mathbf{u}_i - \mathbf{f}_i) \quad , \tag{3.4}$$

where $\tilde{\mathbf{u}}_i$ are the Lagrange multipliers (adjoints). Variation of the Lagrangian with respect to each of the variables then results in:

$$\frac{dL}{d\tilde{\mathbf{u}}_i} = \mathbf{K}\mathbf{u}_i - \mathbf{f}_i = 0 \tag{3.5a}$$

$$\frac{dL}{d\mathbf{u}_i} = \sum_{j=1}^{m} w_{ij}^{md} \mathbf{I}_{ij}^d (\mathbf{u}_{ij}^{md} - \mathbf{I}_{ij}^d \mathbf{u}_i) + \sum_{j=1}^{m} w_{ij}^{ms} \mathbf{J}_{ij}^s (\mathbf{s}_{ij}^{ms} - \mathbf{I}_{ij}^s \mathbf{s}_i) + \mathbf{K}^t \tilde{\mathbf{u}}_i = 0 \tag{3.5b}$$

$$\frac{dL}{d\alpha_e} = \sum_{i=1}^{n} \tilde{\mathbf{u}}_i^t \frac{d\mathbf{K}}{d\alpha_e} \mathbf{u}_i = \sum_{i=1}^{n} \tilde{\mathbf{u}}_i^t \mathbf{K}^e \mathbf{u}_i \quad , \tag{3.5c}$$

where $\mathbf{J}_{ij}^s$ denotes the relationship between the displacements and strains (i.e. the derivatives of the displacement field on the finite element mesh and the location $\mathbf{x}_j$).
The consequences of this rearrangement are profound:

- The gradient of L, I with respect to α may be obtained by solving n forward and adjoint problems; i.e.
- Unlike finite difference methods, which require at least n forward problems per design variable, the number of forward and adjoint problems to be solved is **independent of the number of variables used for** α (!);
- Once the n forward and adjoint problems have been solved, the cost for the evaluation of the gradient of each design variable α_e only involves the degrees of freedom of the element, i.e. is of complexity $O(1)$;
- For most structural problems $\mathbf{K} = \mathbf{K}^t$, so if a direct solver has been employed for the forward problem, the cost for the evaluation of the adjoint problems is negligible;
- For most structural problems $\mathbf{K} = \mathbf{K}^t$, so if an iterative solver is employed for the forward and adjoint problems, the preconditioner can be re-utilized.

3.2 OPTIMIZATION STEPS

An optimization cycle using the adjoint approach is composed of the following steps:
For each force/measurement pair i:

- With current α: solve for the displacements $\rightarrow \mathbf{u}_i$
- With current α, $\mathbf{u}_i$ and $\mathbf{u}_{ij}^{md}, \mathbf{s}_{ij}^{ms}$: solve for the adjoints $\rightarrow \tilde{\mathbf{u}}_i$
- With $\mathbf{u}_i, \tilde{\mathbf{u}}_i$: obtain gradients $\rightarrow I_{,\alpha}^i = L_{,\alpha}^i$

Once all the gradients have been obtained:

- Sum up the gradients $\rightarrow I_{,\alpha} = \sum_{i=1}^n I_{,\alpha}^i$
- If necessary: smooth gradients $\rightarrow I_{,\alpha}^{smoo}$
- Update $\alpha_{new} = \alpha_{old} - \gamma I_{,\alpha}^{smoo}$.

Here γ is a small stepsize that can be adjusted so as to obtain optimal convergence (e.g. via a line search method). Further details of the method (interpolation of displacements and strains, choice of weights, smoothing of gradients, optimization techniques, implementation in black-box solvers, etc.) are described in.[2,3,24]

IV. ZOOMING IN

While running many testcases, the observation was made that a rough definition of the weakened region is often obtained after a few iterations. It then takes a considerable time to 'sharpen' these weakened regions over the course of many iterations. This led to the development of two techniques to 'zoom in' to the weakened regions. The first technique simply removes the regions that are not weakened from further consideration. The second assumes that one can define a coarsening by regions of the finite element mesh; the weakening is obtained on each subregion; once this has converged, all elements are considered for weakening. In both cases, the number of variables to be optimized is reduced, leading to faster convergence.

A. Z1: Removal of Active Elements

The idea here is to remove the regions that are not weakened (or that do not change from an initial state) from further consideration. A simple algorithmic implementation is by marking appropriately the elements whose strength factor is no longer considered. In the present case, all elements whose strength factor is larger than a threshold (e.g. $\alpha > 0.95$) were marked. The gradient of the cost function in these elements is then set to zero during subsequent iterations.
The obvious danger of deactivating zones is that during future iterations, the strength factor may vary. In order to leave some room for future changes, the elements that fall inside a number of 'safety layers' surrounding active elements are also kept as active. In this way, the active region can 'regrow'. The number of safety layers is typically set to 2-3. The number of optimization steps during which the active set is kept fixed is presently prescribed by the user. However, the line search algorithm usually terminates before as the stepsize becomes very small. The elements/gradients are then again marked as active/inactive, and the optimization continues.

B. Z2: Coarsening by Regions

In this case contiguous (and ideally convex/spherical) regions of elements are defined for the fine finite element mesh. The weakening is considered as constant in each of these regions. During each iteration, once the gradients have been obtained at the element level, they are averaged in each region (typically via volume averaging, although other options could be envisioned). This implies that the optimization space is only of the order of regions, not of the order of elements. This leads to very fast convergence. Once the weakening in each region is obtained (or the iteration stalls), all elements are considered for weakening. Obviously, one could envision a series of coarsenings as is done for multigrid methods. For the moment, we have only explored this 2-step procedure.

C. Z3: Combination of Z1 and Z2

It is clear that both methods can easily be combined.

V. EXAMPLES

All the numerical examples were carried out using two finite element codes. The first, FEELAST,[19] is a finite element code based on simple linear (truss), triangular (plate) and tetrahedral (volume) elements with constant material properties per element that only solves the linear elasticity equations. The second, CALCULIX,[14] is a general, open source finite element code for structural mechanical applications with many element types, material models and options. The optimization loops were steered via a simple shell-script for the adjoint-based gradient descent method. In all cases, a 'target' distribution of $\alpha(\mathbf{x})$ was given, together with defined external forces $\mathbf{f}_\Gamma$. The problem was then solved, i.e. the displacements $\mathbf{u}(\mathbf{x})$ and strains $\mathbf{s}(\mathbf{x})$ were obtained and recorded at the 'measurement locations' $\mathbf{x}_j,\ j = 1, m$. This then yielded the 'measurement pair' $\mathbf{f}, \mathbf{u}_j,\ j = 1, m$ or $\mathbf{f}, \mathbf{s}_j,\ j = 1, m$ that was used to determine the material strength distributions $\alpha(\mathbf{x})$ in the field.

5.1 Crane

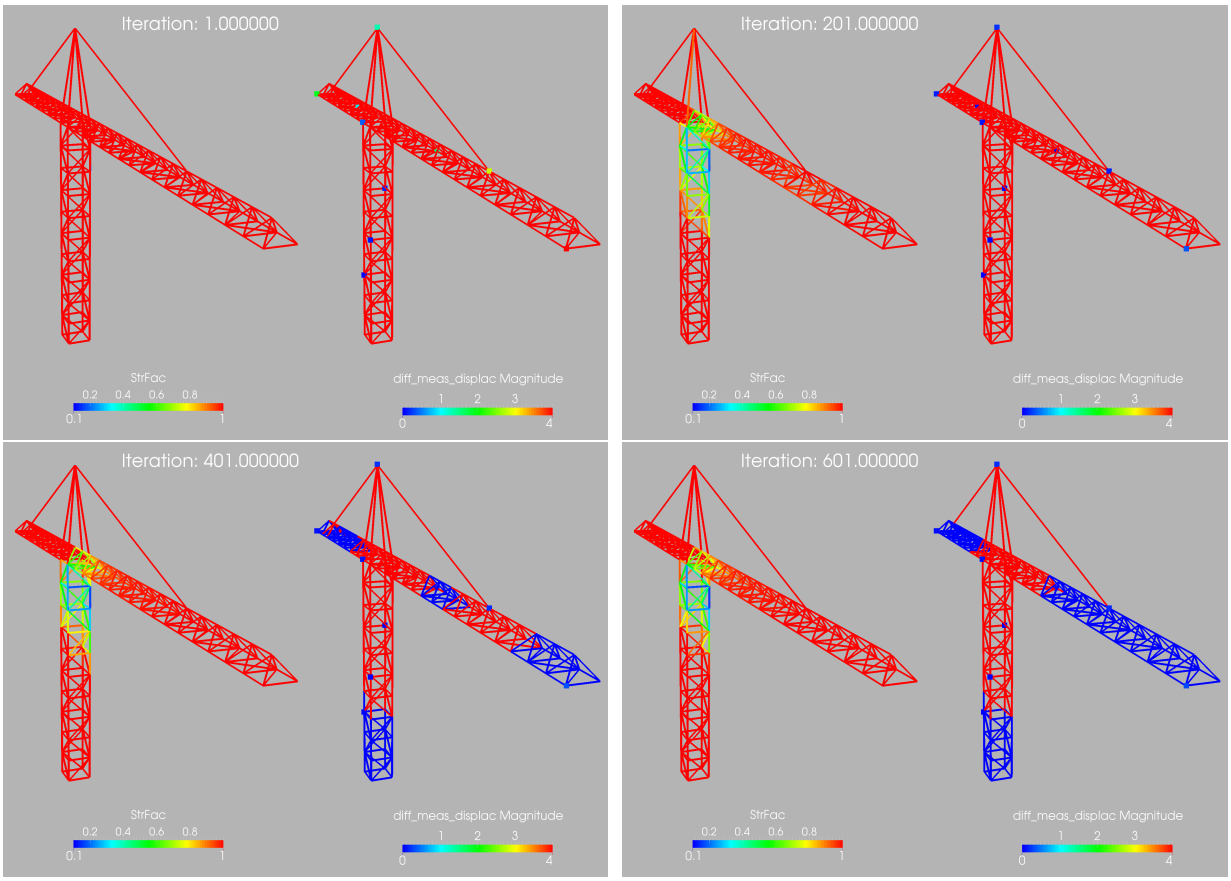

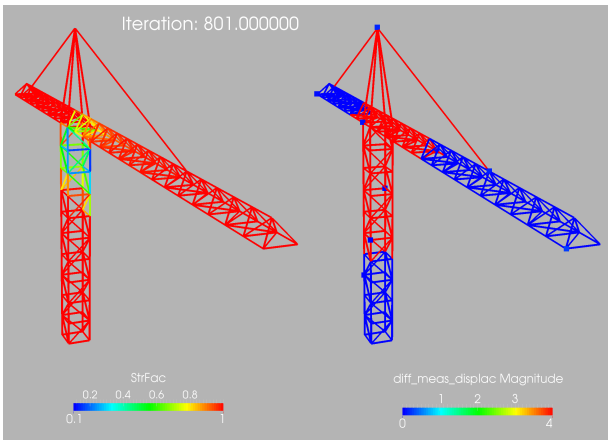

Figures 5.1a-e Crane: Evolution of Strength Factor (Left) and Deactivation Zones (Right)

The case is shown in Figure 5.1 and considers a typical crane used at construction sites. The crane has a height of 1,400 cm, and the arm has a length of 2,500 cm. A typical truss is about 100 cm long and has an area of 5 sqcm. Density, Young's modulus and Poisson rate were set to $\rho = 7.8, E = 2 \cdot 10^{12}, \nu = 0.3$ respectively (all cgs units). The two end points on the arm had loads of $f_y = -2.0 \cdot 10^9$ $gr\ cm/sec^2$ applied, while the two end points on balancing/back part of the arm had loads of $f_y = -1.0 \cdot 10^9$ $gr\ cm/sec^2$. The finite element discretization consisted of 350 linear truss elements. The loads lead to a deformation in the vertical direction $w_y = -18$ cm at the tip of the arm. For this case, only the first zoom method (Z1) was employed. The target weakening is shown on the right of Figure 5f. Figures 5a-e show the strength factor α on the left, and on the right the deactivated zones (blue) and the difference in the absolute value of the displacements at the ten (displacement) measuring points used (which in this case coincide with nodes of the finite element mesh). Figure 5.1f compares the final strength factor obtained (left) and the target strength factor (right), and Figure 5.1g the convergence history of the cost function. Note that these are two curves: the curves with (labelled 'Coar') and without (labelled 'NoCo') zooming are identical for steepest descent and constant stepsize. This behaviour has been noted repeatedly, and is very different than that observed for line searches. It also shows that for this case the gradient in the regions of $\alpha = O(1)$ tends to increase α, something that is not allowed.

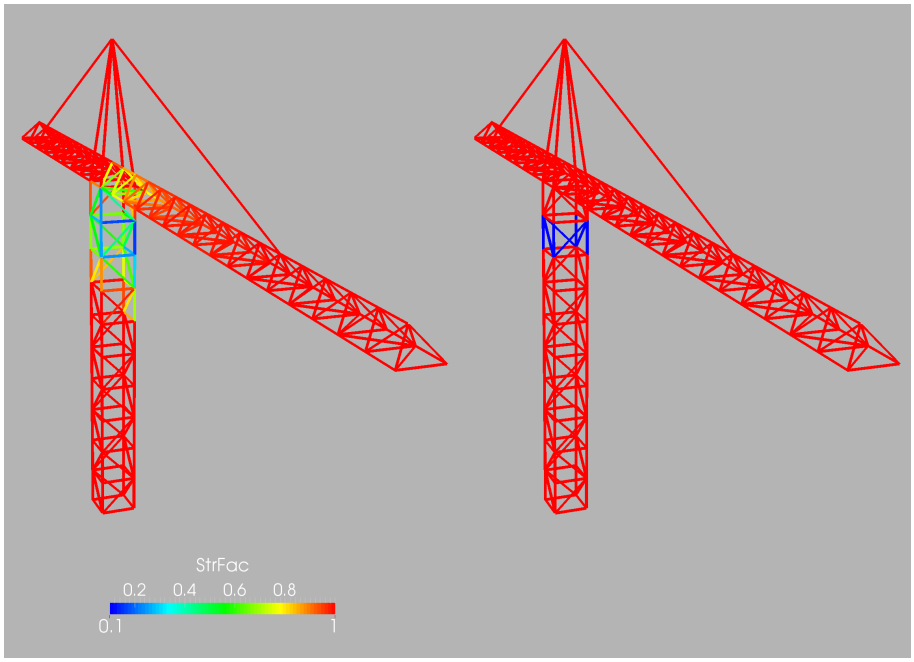

Figure 5.1f Crane: Final Strength Factor (Left) and Target Strength Factor (Right)

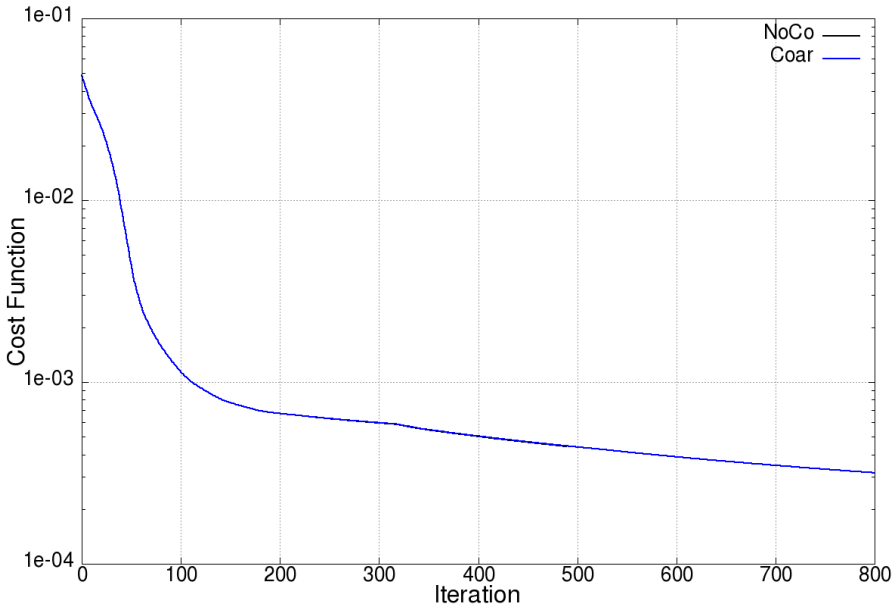

Figure 5.1g Crane: Convergence of the Cost Function

5.2 Plate With Hole

The case is shown in Figures 5.2a,c, and considers a plate with a hole. The plate dimensions are (all units in cgs): $0 \le x \le 60, 0 \le y \le 30, 0 \le z \le 0.1$. A hole of diameter $d = 10$ is placed in the middle $(x = 30, y = 15)$. Density, Young's modulus and Poisson rate were set to $\rho = 7.8, E = 2 \cdot 10^{12}, \nu = 0.3$ respectively. The left boundary of the plate is assumed clamped ($\mathbf{u} = 0$), while a horizontal load of $q = (10^5, 0, 0)$ was prescribed at the right end. A small region of weakened material was specified. A total of 14 measuring points for displacements were specified. These are shown in Figures 5.2a,c as the white dots. Two grids were considered, with 174 (coarse) and 2,596 (fine) linear plain stress finite elements respectively. For this case, only zoom method Z1 was employed. Figures 5.2a,c show the inactive (blue) and active region (red), as well as the strength factor, as the (outer, i.e. zooming in) iterations progress. The convergence history of the cost function for the two grids is displayed in Figures 5.2b,d. Notice that the original optimization procedure (labelled 'NoRed') stalls after 50-60 iterations (the stepsize of the line search falls below a preset tolerance), while with zooming (labelled 'Reduc') a much lower cost function value can be achieved, i.e. a considerable improvement in convergence.

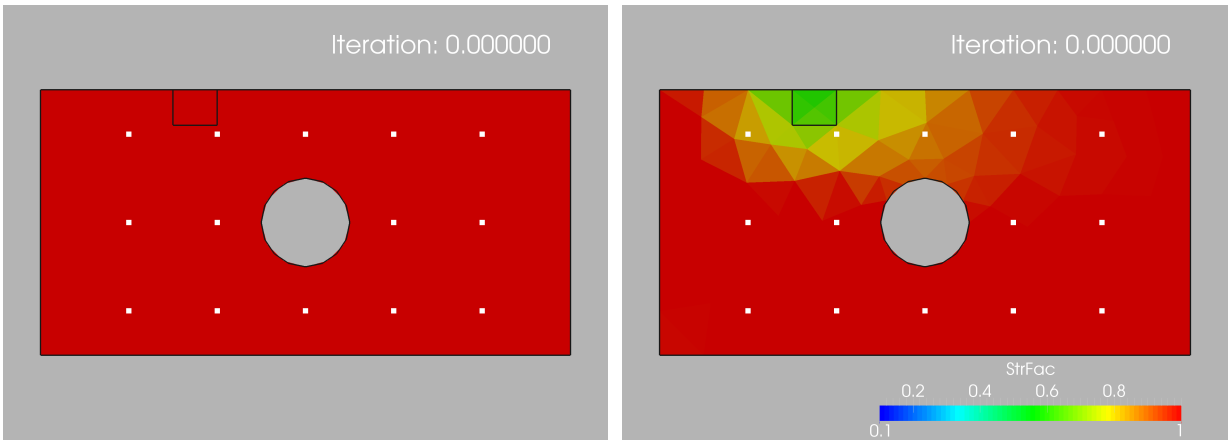

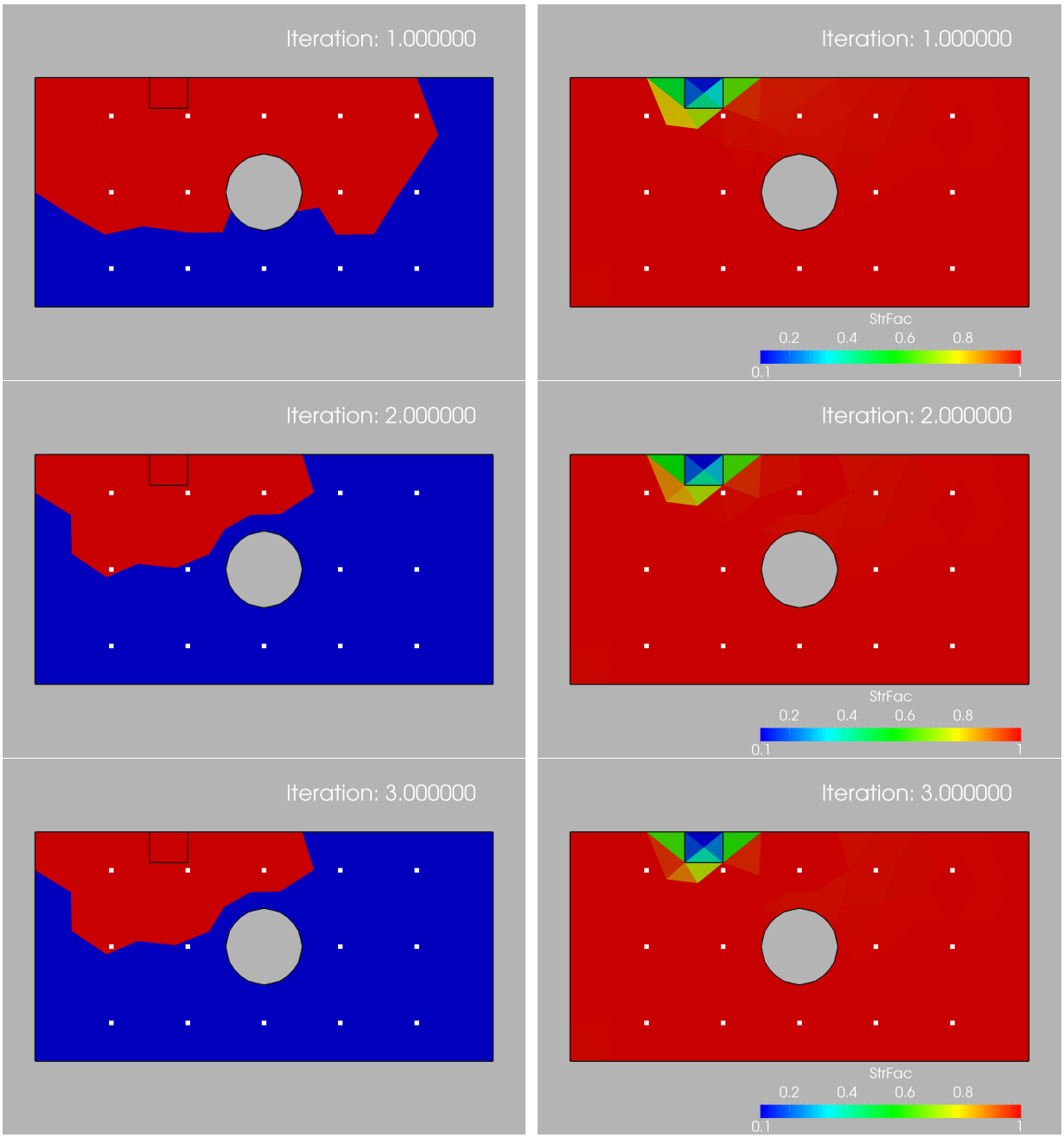

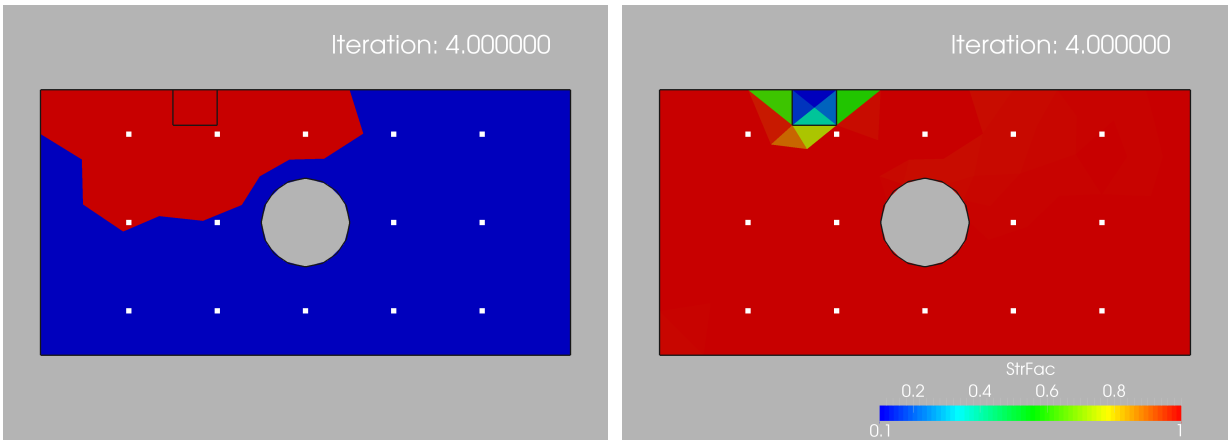

Figure 5.2a Plate With Hole: Coarse Mesh

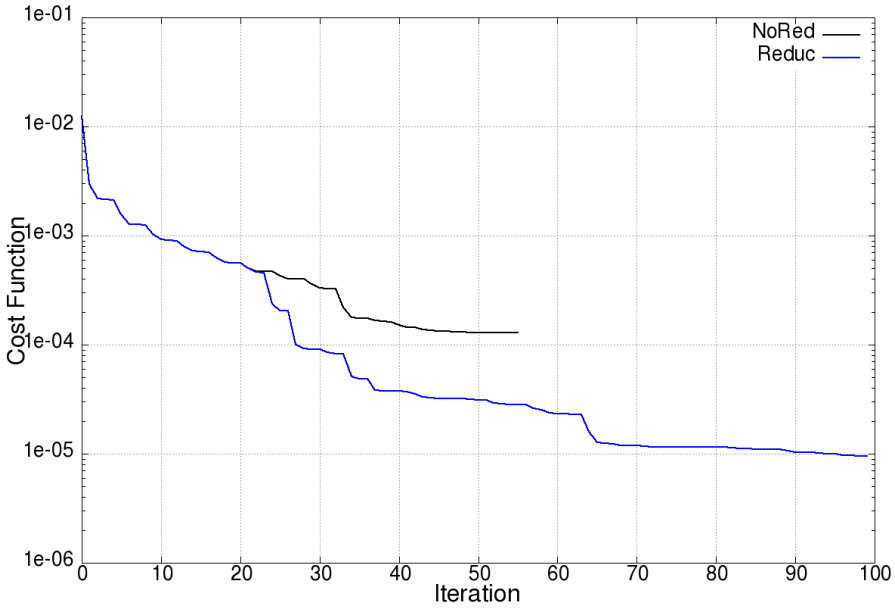

Figure 5.2b Plate With Hole: Convergence History for Coarse Mesh

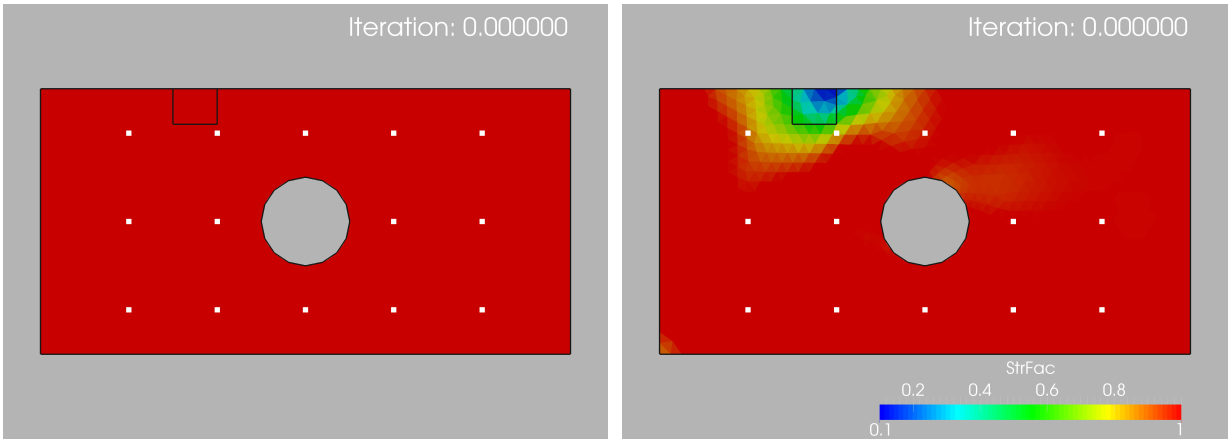

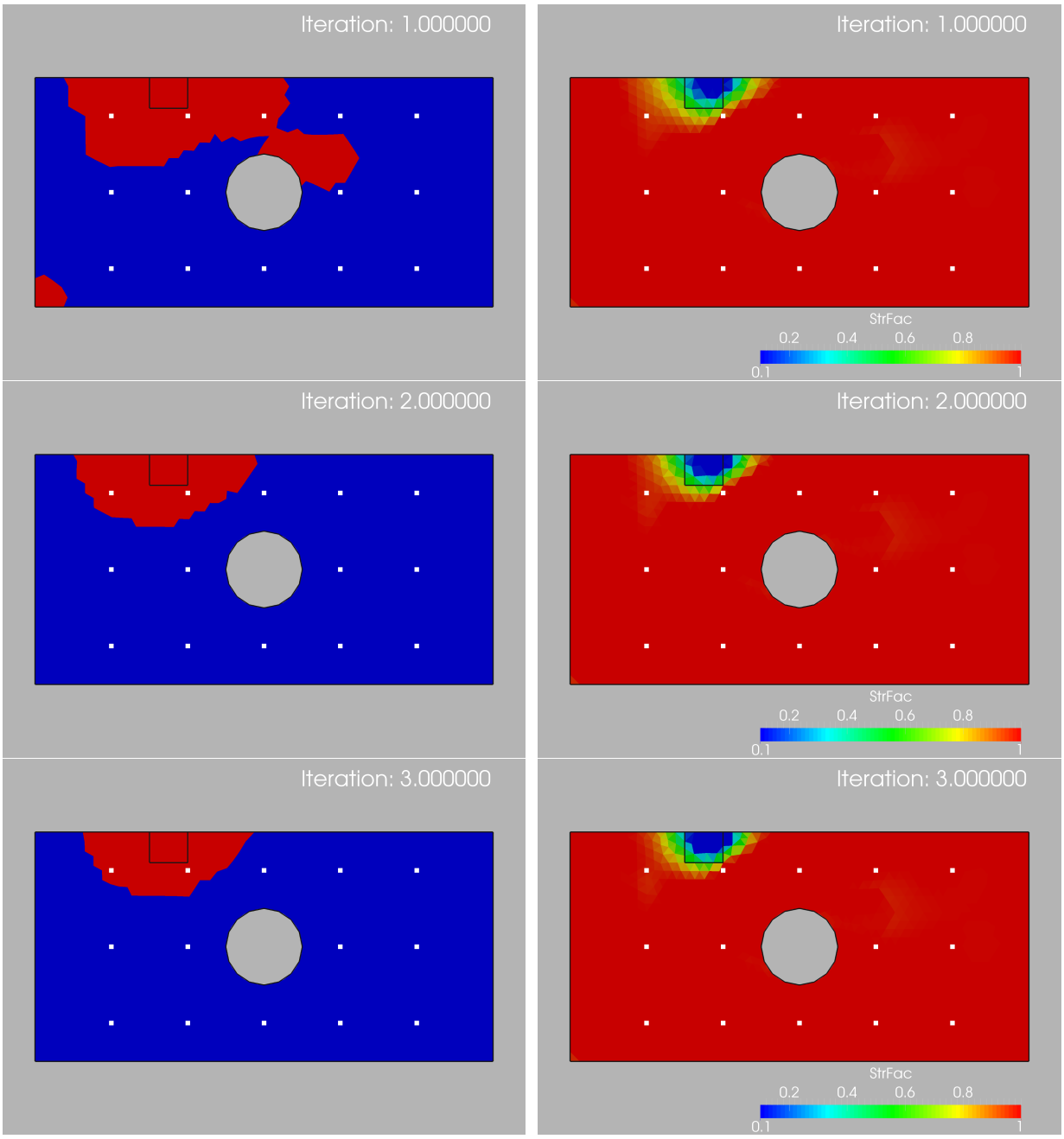

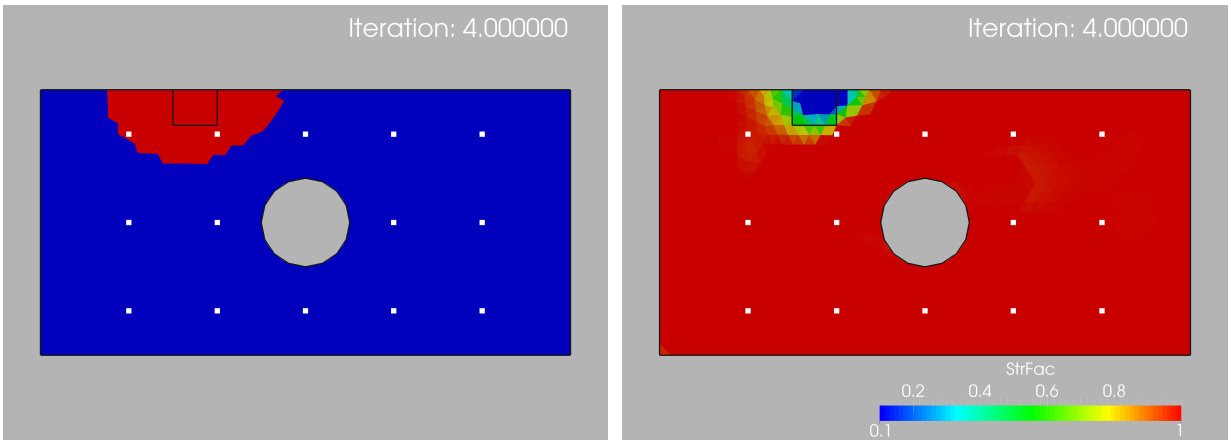

Figure 5.2c Plate With Hole: Fine Mesh

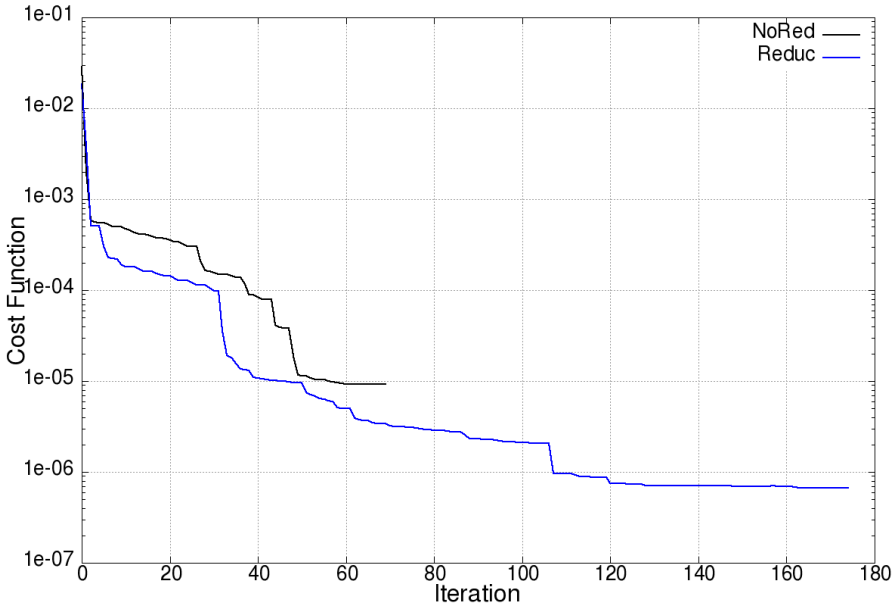

Figure 5.2d Plate With Hole: Convergence History for Fine Mesh

5.3 Plate With Hole

The case is shown in Figures 5.3a,b and considers the same plate as before. However, in this case only zoom method Z2 was employed, together with a simple steepest descent method with constant stepsize. The grouping, shown in Figure 5.3a, was obtained using an advancing front method, and was employed for the first 20 iterations. The strength factor in each element, as well as the difference between the measured and computed displacements is shown in Figures 5.3b. The grouping is clearly visible at iteration 10.

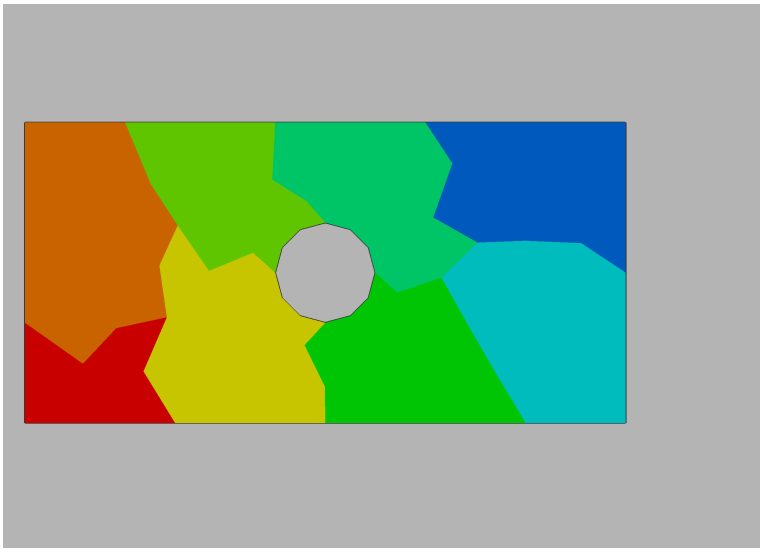

Figure 5.3a Plate With Hole: Grouping of Elements

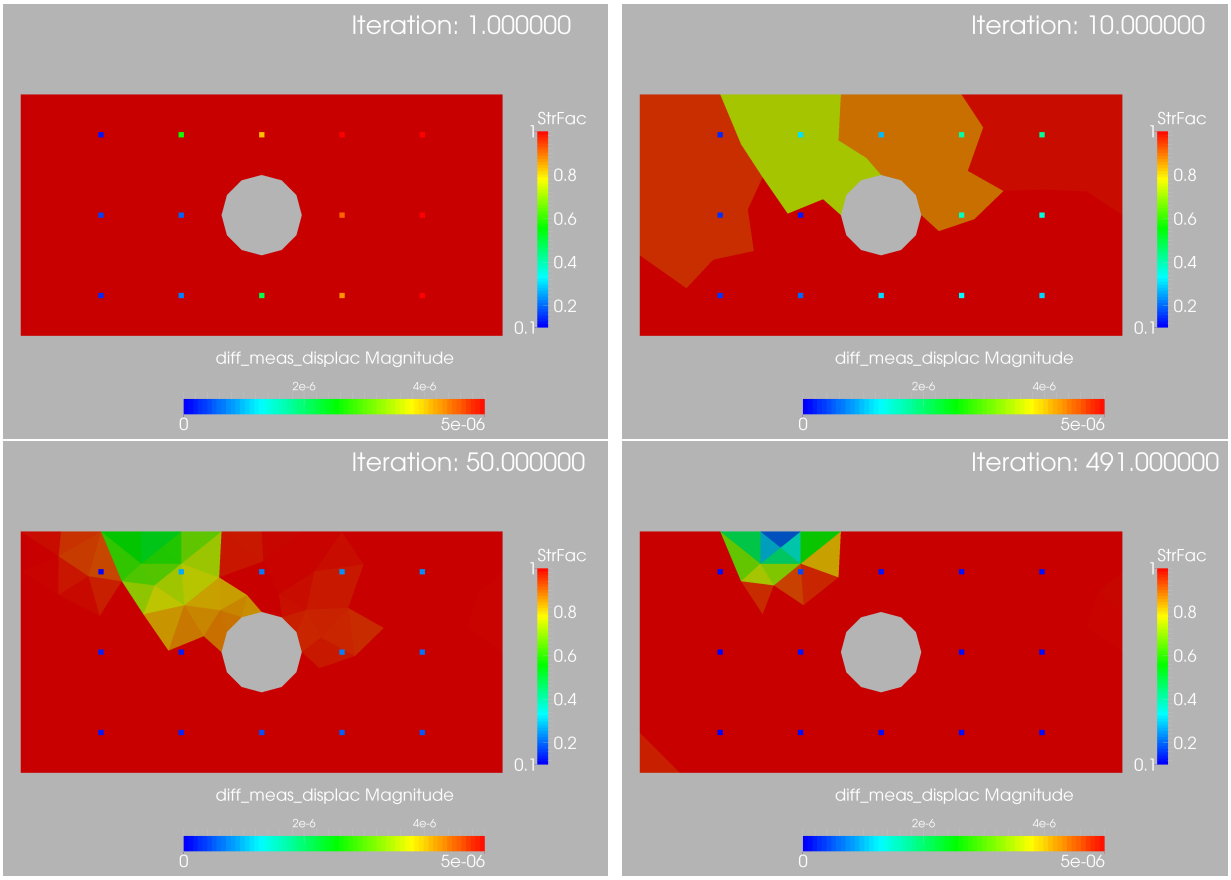

Figure 5.3b Plate With Hole: Evolution of Strength Factor and Difference Between Measurements and Calculations

The convergence history of the cost function is displayed in Figures 5.3c. The difference between the blue and the red curve is the number of initial iterations before switching from grouping of strength factors to individual element strength factors.

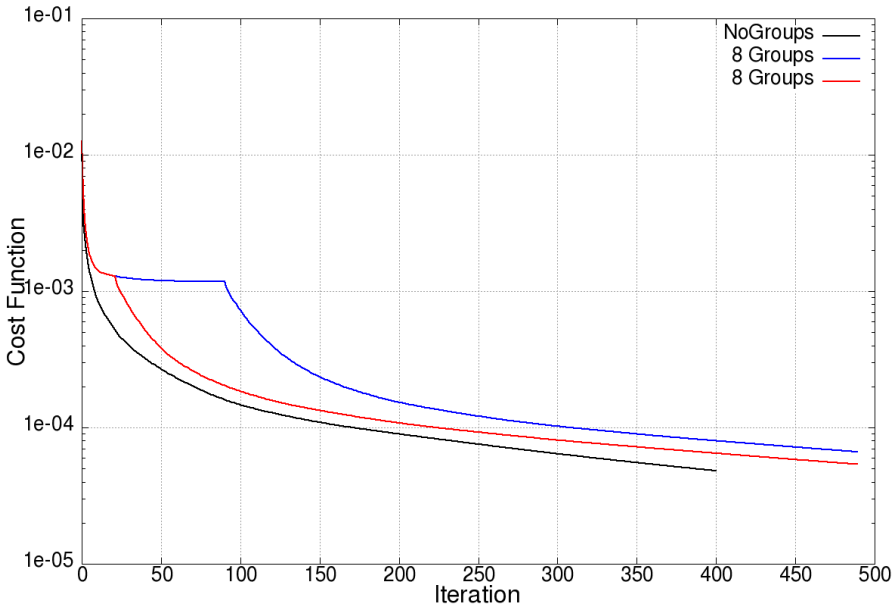

Figure 5.3c Plate With Hole: Convergence History

5.4 Wind Turbine Blade

The case is shown in Figures 5.4a and considers a blade that was produced via additive manufacturing. Density, Young's modulus and Poisson rate were set to $\rho = 7.8, E = 2 \cdot 10^{12}, \nu = 0.3$ (all units in cgs) respectively. 203,229 linear, tetrahedral elements were used. Figures 5.4b,c show details of the mesh. The complete base of the blade is assumed clamped ($\mathbf{u} = 0$), while a load was prescribed on the faces at the tip. The small region of weakened material that was specified is shown in Figure 5.4d, together with some of the 23 measuring points for displacements that were specified. For this case, only zoom method Z1 was employed, together with a line search. Figure 5.4e shows the strength factor [left], as well as the inactive (blue) and active region (red) [right] as the (outer, i.e. zooming in) iterations progress. The convergence history of the cost function is displayed in Figures 5.4f. Note that: a) In every step, the optimization algorithm 'stalls', i.e. can not proceed further as the stepsize falls below a preset tolerance, but the zooming allows further steps; b) Even though the cost function barely diminishes, a marked improvement in the definition of the recovered weakened region is observed when zooming is applied; c) The presence of singularities introduced by the sharp corners at the base 'pollute' the final result.

Figure 5.4a Blade Geometry

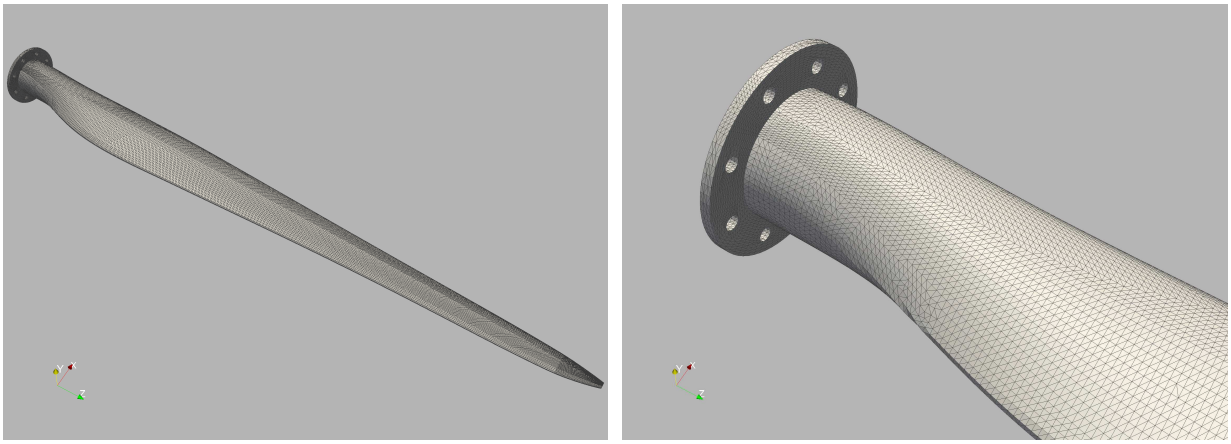

Figure 5.4b,c Blade: Surface of Mesh

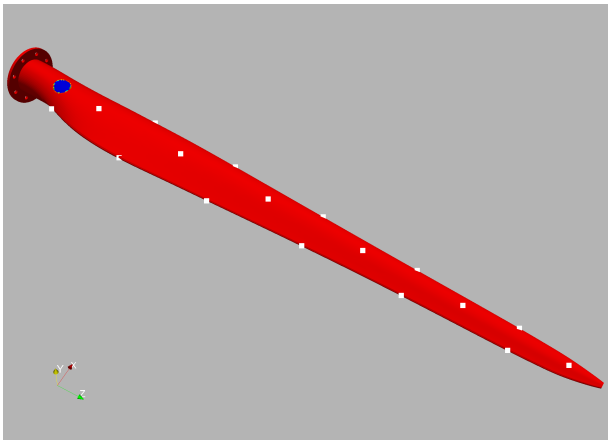

Figure 5.4d Weakened Region and Measurement Points

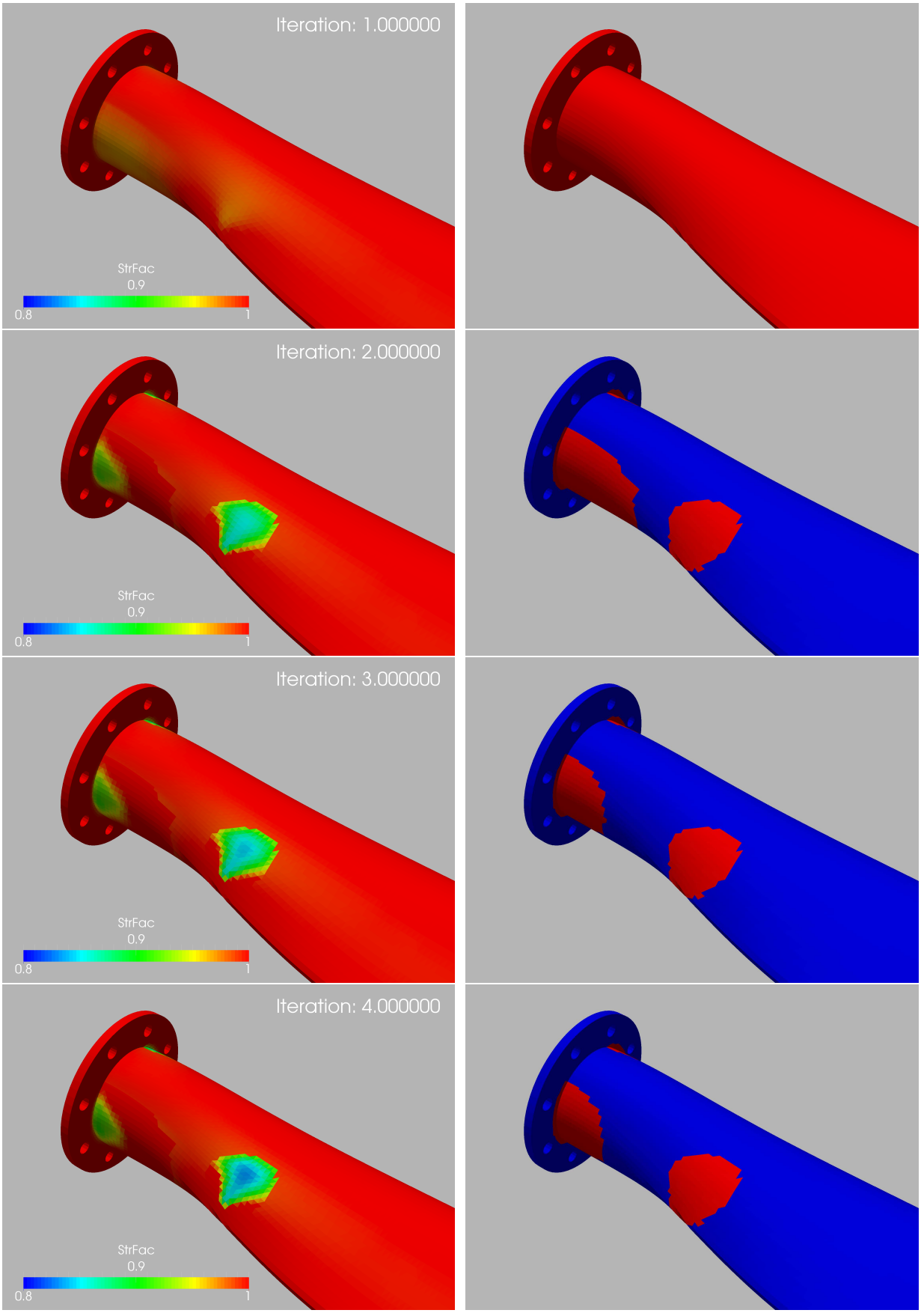

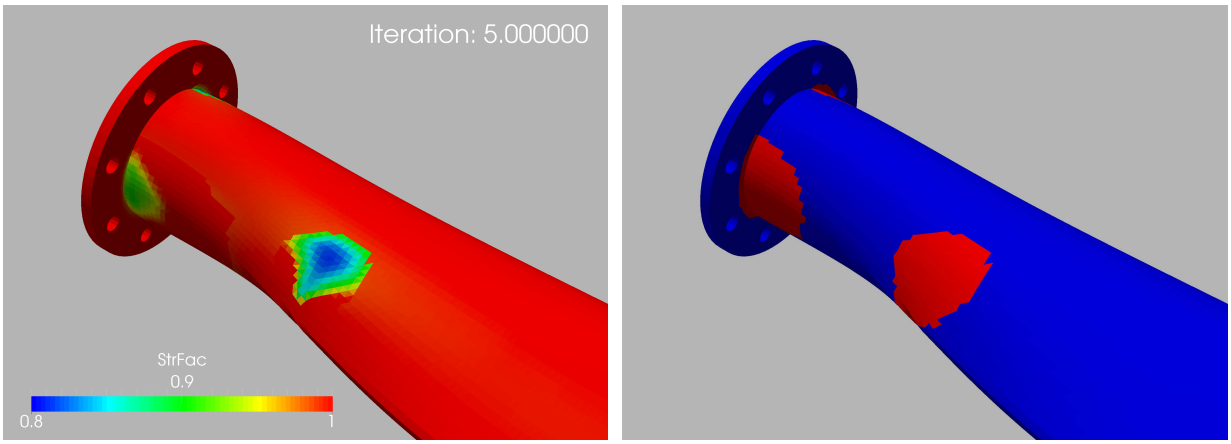

Figure 5.4e Blade: Evolution of Strength Factor and Active Region

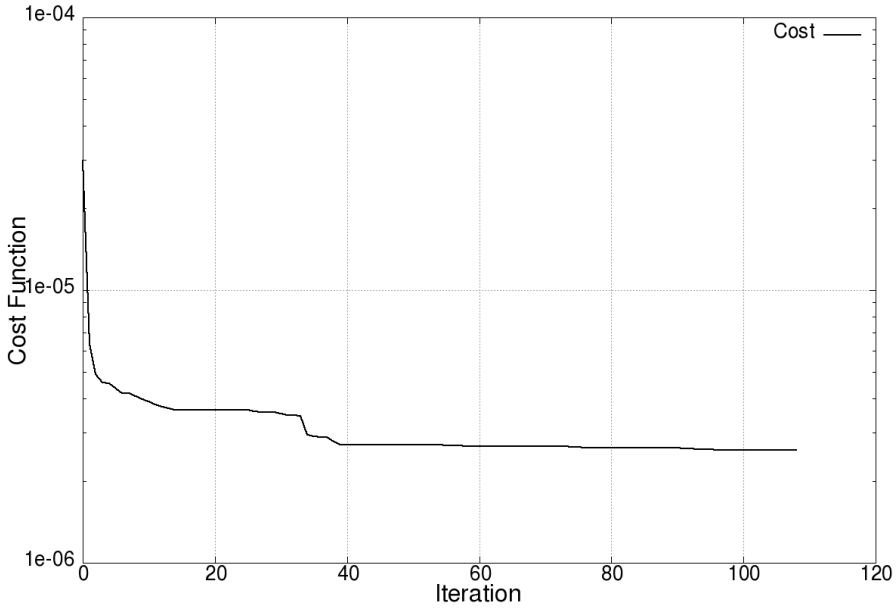

Figure 5.3f Blade: Convergence History

VI. CONCLUSIONS AND OUTLOOK

An adjoint-based procedure to determine weaknesses, or, more generally, the material properties of structures has been improved by implementing two techniques to progressively reduce the regions considered as weakened. In this way, the number of degress of freedom that are being optimized is reduced, leading to faster convergence and a better definition or 'sharpening' of the weakened region.
Several examples show the viability, accuracy and efficiency of the proposed methodology.
Many questions remain open, of which we just mention some obvious ones:

- Will these techniques work for nonlinear problems ?
- Which sensor resolution is required to obtain reliable results ?
- Will these techniques work under uncertain measurements ?[3,6]
- Can one detect faulty sensors in a systematic way ?
- Which are the best optimization techniques for this class of problems ?

VII. ACKNOWLEDGEMENTS

This work is partially supported by NSF grant DMS-2408877, Air Force Office of Scientific Research (AFOSR) under Award NO: FA9550-22-1-0248, and Office of Naval Research (ONR) under Award NO: N00014-24-1-2147. The first author gratefully acknowledges the support of the TU Braunschweig for four biweekly stays at the Institute of Structural Analysis, that led to the development of the techniques described in this paper. Partial funding was also provided by the the Technical University of Munich Institute for Advanced Study. This work was also partially supported by the Deutsche Forschungsgemeinschaft (DFG, German Research Foundation) under German's Excellence Strategy - EXC 2163/1 - Sustainable and Energy Efficient Aviation - Project-ID 390881007.

References

[1]American Institute of Aeronautics and Astronautics (AIAA), Digital Engineering Integration Committee. Digital Twin: Definition and Value; *AIAA and AIA Position Paper* (2020). https://www.aiaa.org/docs/default-source/uploadedfiles/ issues-and-advocacy/policy-papers/digital-twin-institute-position-paper-(december-2020).pdf.

[2]F.N. Airaudo, R. Löhner, R. Wüchner and H. Antil - Adjoint-Based Determination of Weaknesses in Structures; *Comp. Meth. Appl. Mech. Eng.* 417, A, 116471 (2023).

[3]F.N. Airaudo, H. Antil, R. Löhner and U. Rakhimov - On the Use of Risk Measures in Digital Twins to Identify Weaknesses in Structures; *AIAA*-2024-2622 (2024). https://doi.org/10.2514/6.2024-2622

[4]N.F. Alkayem, M. Cao, Y. Zhang, M. Bayat and Z. Su - Structural Damage Detection Using Finite Element Model Updating With Evolutionary Algorithms: A Survey; *Neural Comput. Applic.* 30, 389411 (2018).

[5]H. Antil, D.P. Kouri, M.-D. Lacasse and D. Ridzal (eds.) - *Frontiers in PDE-Constrained Optimization*; IMA Volumes in Mathematics and its Applications 163, Springer Verlag (2018).

[6]H. Antil, S. Dolgov and A. Onwunta - State-Constrained Optimization Problems Under Uncertainty: A Tensor Train Approach; arXiv:2301.08684v1 math.OC (2023). https://onlinelibrary.wiley.com/doi/full/10.1002/nla.2481

[7]H. Antil - Mathematical Opportunities in Digital Twins (MATH-DT); *arXiv preprint arXiv:2402.10326* (2024).

[8]T. Borrvall and J. Petersson - Topology Optimization of Fluids in Stokes Flow; *Int. J. Num. Meth. Fluids* 41(1), 77-107 (2003).

[9]M. Botz, A. Emiroglu, K. Osterminski, M. Raith, R. Wüchner and C. Grosse - Überwachung und Modellierung der Tragstruktur von Windenergieanlagen - Beitrag zu einem Digitalen Zwilling; *Beton- und Stahlbetonbau* 115, 342-354 (2020).

[10]G. Bunting, S.T. Miller, T.F. Walsh, C.R. Dohrmann and W. Aquino - Novel Strategies for Modal-Based Structural Material Identification; *Mechanical Systems and Signal Processing* 149, 107295 (2021).

[11]P. Cawley and R.D. Adams - The Location of Defects in Structures From Measurements of Natural Frequencies; *J. Strain Anal. Eng. Des.* 4, 4957 (1979).

[12]L. Chamoin, P. Ladevèze and J. Waeytens - Goal-Oriented Updating of Mechanical Models Using the Adjoint Framework; *Comp. Mech.* 54, 6, 1415-1430 (2014).

[13]F. Chinesta, E. Cueto, E. Abisset-Chavanne, J.L. Duval and F.E. Khaldi - Virtual, Digital and Hybrid Twins: A New Paradigm in Data-Based Engineering and Engineered Data; *Arch. Comput. Meth. Eng.* 27, 105134 (2020).

[14]G. Dhondt- *CalculiX CrunchiX USERS MANUAL Version 2.20* (2022).

[15]S. Grabke, F. Clauss, K.-U. Bletzinger, M.A. Ahrens, P. Mark and R. Wüchner - Damage Detection at a Reinforced Concrete Specimen with Coda Wave Interferometry; *Materials* 14:5013 (2021).

[16]S. Grabke,K.-U. Bletzinger and R. Wüchner - Development of a Finite Element-Based Damage Localization Technique for Concrete by applying Coda Wave Interferometry; *Engineering Structures* 269:114585 (2022).

[17]A. Kilikevicius, D. Bacinskas, J. Selech, K. Kilikeviciene, D. Vainorius, D. Ulbrich, J. Matijosius and D. Romek - The Influence of Different Loads on the Footbridge Dynamic Parameters, *Symmetry* 12, 657 (2020). doi:10.3390/sym12040657

[18]H. Kim and H. Melhem - Damage Detection of Structures by Wavelet Analysis; *Eng. Struct.* 26, 347362 (2004).

[19]R. Löhner - FEELAST User's Manual (2023).

[20]P. Ladevèze, D. Nedjar and M. Reynier - Updating of Finite Element Models Using Vibration Tests; *AIAA J.* 32, 7, 1485-1491 (1994).

[21]B.S. Lazarov and O. Sigmund - Filters in Topology Optimization Based on HelmholtzType Differential Equations; *Int. J. Num. Meth. Engineering* 86(6), 765-781 (2011).

[22]R. Löhner - *Applied CFD Techniques, Second Edition*; J. Wiley & Sons (2008).

[23]R. Löhner and H. Antil - Determination of Volumetric Material Data from Boundary Measurements: Revisiting Calderon's Problem; *Int. J. Num. Meth. Heat and Fluid Flow* 30, 11, 4837-4863 (2020). DOI: 10.1108/HFF-12-2019-0931.

[24]R. Löhner, F.N. Airaudo, H. Antil, R. Wüchner, F. Meister and S. Warnakulasuriya - High-Fidelity Digital Twins: Detecting and Localizing Weaknesses in Structures; *Int. J. Num. Meth. Eng.* 125, 21, e7568 (2024). https://doi.org/10.1002/nme.7568

[25]D. Di Lorenzo, V. Champaney, C. Germoso, E. Cueto, and F. Chinesta - Data Completion, Model Correction and Enrichment Based on Sparse Identification and Data Assimilation; *Appl. Sci.* 12, 7458 (2022). https://doi.org/10.3390/app12157458

[26]N.M. Maia, J.M.N. Silva and R. Sampaio - Localization of Damage Using Curvature of the Frequency Response Functions; in *Proc. 15th Int. Modal Analysis Conference Society of Experimental Mechanics*, Orlando, FL, USA, 36 February (1997).

[27]L. Mainini and K. Willcox - Surrogate Modeling Approach to Support Real-Time Structural Assessment and Decision Making; *AIAA J.* 53, 16121626 (2015).

[28]A. Mirzaee, R. Abbasnia and M. Shayanfar - A Comparative Study on Sensitivity-Based Damage Detection Methods in Bridges; *Shock and Vibration* (2015).

[29]S.C. Mohan, D.K. Maiti and D. Maity - Structural Damage Assessment Using FRF Employing Particle Swarm Optimization; *Appl. Math. Comput.* 219, 1038710400 (2013).

[30]National Academies of Sciences, Engineering, and Medicine - Foundational Research Gaps and Future Directions for Digital Twins; *ISBN* 978-0-309-70042-9 (2023). https://doi.org/10.17226/26894, https://nap.nationalacademies.org/catalog/26894/foundational-research-gaps-and-future-directions-for-digital-twins

[31]T. Planès and E. Larose - A Review of Ultrasonic Coda Wave Interferometry In Concrete; *Cem. Concr. Res.* 53 (2013).

[32]G. Puel and D. Aubry - Using Mesh Adaption for the Identification of a Spatial Field of Material Properties; *Int. J. Num. Meth. Eng.* 88, 3, 205-227 (2011).

[33]M. Rucka and K. Wilde - Application of Continuous Wavelet Transform in Vibration Based Damage Detection Method for Beams and Plates; *J. Sound Vib.* 297, 536550 (2006).

[34]M. Salloum and D.B. Robinson - Optimization of Flow in Additively Manufactured Porous Columns with Graded Permeability; *AIChE Journal* 68(9), e17756 (2022).

[35]D.T. Seidl, A.A. Oberai and P.E. Barbone - The Coupled Adjoint-State Equation in Forward and Inverse Linear Elasticity: Incompressible Plane Stress; *Comp. Meth. Appl. Mech. Eng.* 357, 112588 (2019).

[36]J.C. Simo and T.J.R. Hughes - *Computational Inelasticity*; Springer, New York (1997).

[37]F. Troltzsch - *Optimal Control of Partial Differential Equations: Theory, Methods and Applications*; American Mathematical Society (2010).

[38]K. Willcox, O. Ghattas and K. Soga - Crosscutting Research Needs Digital Twins (2024); https://www.santafe.edu/events/crosscutting-research-needs-digital-twins

[39]O.C. Zienkiewicz and R.L. Taylor - *The Finite Element Method*; McGraw-Hill Book Company (1989).